HHS Public Access

Author manuscript

J Invest Dermatol. Author manuscript; available in PMC 2019 March 01.

Published in final edited form as:

J Invest Dermatol. 2018 March ; 138(3): 697–703. doi:10.1016/j.jid.2017.09.031.

The Physicochemical Basis of Clofazimine-Induced Skin Pigmentation

Mikhail D. Murashov[1], **Vernon LaLone**[1], **Phillip M. Rzeczycki**[1], **Rahul K. Keswani**[1], **Gi S. Yoon**[1], **Sudha Sud**[1], **Walajapet Rajeswaran**[2], **Scott Larsen**[2], **Kathleen A. Stringer**[3], and **Gus R. Rosania**[1]

[1]Department of Pharmaceutical Sciences, University of Michigan, Ann Arbor, Michigan, USA

[2]Department of Medicinal Chemistry, University of Michigan, Ann Arbor, Michigan, USA

[3]Department of Clinical Pharmacy, University of Michigan, Ann Arbor, Michigan, USA

Abstract

Clofazimine is a weakly basic, FDA-approved antibiotic recommended by the World Health Organization to treat leprosy and multi-drug-resistant tuberculosis. Upon prolonged treatment, clofazimine extensively bioaccumulates and precipitates throughout the organism, forming crystal-like drug inclusions (CLDIs). Because of the drug's red color, it is widely believed that clofazimine bioaccumulation results in skin pigmentation, its most common side effect. To test whether clofazimine-induced skin pigmentation is due to CLDI formation, we synthesized a closely related clofazimine analog that does not precipitate under physiological pH and chloride conditions that are required for CLDI formation. Despite the absence of detectable CLDIs in mice, administration of this analog still led to significant skin pigmentation. In clofazimine treated mice, skin cryosections revealed no evidence of CLDIs when analyzed with a microscopic imaging system specifically designed for detecting clofazimine aggregates. Rather, the reflectance spectra of the skin revealed a signal corresponding to the soluble, free base form of the drug. Consistent with the low concentrations of clofazimine in the skin, these results suggest that clofazimine-induced skin pigmentation is not due to clofazimine precipitation and CLDI formation, but rather to the partitioning of the circulating, free base form of the drug into subcutaneous fat.

Graphical abstract

Corresponding Author's Contact Information: Gus R. Rosania, PhD (Corresponding author), Professor of Pharmaceutical Sciences, University of Michigan College of Pharmacy, 428 Church Street, Ann Arbor, MI 48109, grosania@umich.edu, Phone: 734-358-5661.

Conflict Of Interest: Gus R. Rosania is consulting for Bristol-Myers Squibb.

Introduction

Drug-induced skin pigmentation corresponds to approximately 10-20% of all cases of hyperpigmentation (Dereure, 2001). It can be induced by a wide variety of drugs (i.e. NSAIDs, weakly basic drugs, heavy metals, psychotropic drugs, etc.) through several mechanisms that can involve an accumulation of melanin as a non-specific post-inflammatory change in predisposed individuals that is often worsened by sun exposure; an accumulation of the triggering drug itself and/or reacting with other substances in the skin; and due to deposits of certain heavy metals (i.e. iron) that can cause damage to the dermal vessels (Dereure, 2001). Hyperpigmentation caused by weakly basic drugs (i.e. chloroquine, amiodarone, and clofazimine) is one of the particular interest and importance because approximately 75% of drugs on the market are classified as weak bases (Dereure, 2001, Gallo et al., 2009, Maia et al., 2013, Manallack, 2008, Tang et al., 2015). One of the most extreme examples of weakly basic drugs that causes severe hyperpigmentation is clofazimine, and yet, the basis of clofazimine drug-induced skin pigmentation has never been investigated.

Clofazimine (CFZ) is a weakly basic, very lipophilic, phenazine antibiotic (Arbiser and Moschella, 1995) that has been effectively used to treat leprosy for over 40 years. Curing more than 14 million people worldwide, this drug is on the World Health Organization's (WHO) list of essential medications (World Health Organization, 2014). Furthermore, due to its potent activity against *Mycobacterium tuberculosis*, CFZ is now recommended by WHO as a second line agent against multi-drug resistant tuberculosis (MDR-TB), which is supported by in vitro to animal and human studies (Dooley et al., 2013, Gopal et al., 2013), including a randomized, prospective clinical trial (Tang et al., 2015).

Regardless of the indication, whether it is for leprosy or MDR-TB, studies that have evaluated the clinical efficacy and tolerability of CFZ have reported that skin pigmentation is

the most common and dominating side effect that is observed in more than 94% of the patients (Maia et al., 2013, Tang et al., 2015). Patients may also experience ichthyosis or gastrointestinal symptoms, but at the normal dosage of 50 to 100mg/day, no other major side effects have been reported (Hastings et al., 1988, Jamet et al., 1992, Maia et al., 2013, Singh et al., 2011).

In mice, long term exposure (≥ 8 weeks) to orally administered CFZ has also been associated with extensive pigmentation of skin and internal organs (Abstract Figure) (Baik et al., 2013). Solid drug precipitates accumulate in tissue macrophages, forming Crystal-Like Drug Inclusions (CLDIs) that are most abundant in liver and spleen (Baik and Rosania, 2011, 2012, Baik et al., 2013). CLDIs have also been reported in humans treated with the drug (Belaube et al., 1983, Sukpanichnant et al., 2000). Once inside the cell, these biocrystals display robust stability and remain in the body long after the discontinuation of treatment (Baik et al., 2013).

Microscopically, CLDIs show strong fluorescence in the Cy5 channel (650 nm excitation / 670 nm emission) (Keswani et al., 2015b). Furthermore, CLDIs are also detected via diattenuation due to the interaction of these supramolecular ordered structures with polarized light (Rzeczycki et al., 2017). Analysis of isolated CLDIs revealed chemical and structural properties that are consistent with that of a specific CFZ hydrochloride salt (CFZ-HCl) polymorph (Keswani et al., 2015a).

Due to the fact that orally administered CFZ has been associated with massive intracellular accumulation of CLDIs and strong red pigmentation of macrophage-containing organs (Baik et al., 2013), we hypothesized that skin pigmentation is associated with CLDI bioaccumulation in macrophages. To test this hypothesis, we identified a closely related CFZ analog that does not form CLDIs and determined its ability to cause skin pigmentation. In addition, we characterized the spectral properties of CFZ-induced skin pigmentation and conducted detailed microscopic analysis to identify the optical signature of CLDIs or precipitated CFZ hydrochloride in the skin of drug treated mice.

Results And Discussion

In our previous study, we synthesized a focused library of phenazine derivatives of CFZ and assayed their bioaccumulation and self-assembly properties in RAW264.7 macrophages and Madin-Darby Canine Kidney (MDCK) epithelial cells (Min et al., 2015). As the result, three derivatives yielded cellular staining patterns comparable in morphology and intensity to those of CFZ; one of them was CFZ analog 568 (Min et al., 2015), which was chosen to be used as an experimental control for this study. Comparison of key physicochemical properties between CFZ and this analog revealed minor differences in molecular weights, physiologically relevant pKa values, and partition coefficients (logP and logD at pH 7.4) (Table 1).

Based on spectrophotometric comparison, absorbance profiles of CFZ and the 568 analog were nearly identical for both free base and salt forms (Figure 1b). Both compounds exhibited strong absorbance in UV region at 285nm due to their phenazine backbones; free

base forms showed maximum visible absorbance at 450nm, while the salt forms shifted the visible absorbance peak to 495nm, which is consistent with our previous study (Min et al., 2015).

Next, an *in vitro* precipitation assay that mimics the *in vivo* conditions that leads to CLDI formation was developed to screen for CFZ derivatives that do not form CLDIs. The rationale behind the assay is that CLDIs form by the precipitation of CFZ in the acidic lysosomal microenvironment (pH 4.5) and the formation of a hydrochloride salt in the presence of physiological sodium chloride concentrations. Thus, a pH of 4.5 and chloride concentration of 100mM were chosen to mimic the lysosomal environment (Stauber and Jentsch, 2013). Furthermore, to recapitulate lipophilic drug partitioning within lysosome membranes, cetrimonium bromide (CTAB) was used as a bio-relevant surfactant because it does not interfere with absorbance at 285nm – the UV wavelength of detection for phenazine derivatives (Figure 1b). The optimal concentration of CTAB was determined based on calculated molar solubilization ratio between CFZ and CTAB at pH 4.5 (data not shown) (Chakraborty et al., 2009). Finally, this novel assay was calibrated so the presence of chloride would act as the driving force for the formation of hydrochloride salt. For this, two conditions were employed: Solution A (no chloride) and Solution B (100mM chloride). The precipitation was measured as the decrease in absorbance in 285nm wavelength that correlated with the drug concentration in the solution resulting from precipitation.

By screening the CFZ derivatives using the aforementioned assay, we identified the 568 analog as the most closely related CFZ derivative that did not precipitate out in the lysosomal microenvironment. CFZ and 568 share similar chemical structures (Figure 1a), spectral properties (Figure 1b), physicochemical characteristics (Table 1), and both can be solubilized by detergent in the absence of chloride due to the fact that CFZ and 568 remained soluble in solution A (no chloride) to similar extent as in DMSO. Nevertheless, the 568 analog remains in solution in the presence of physiological chloride concentrations (solution B - 100mM chloride), while CFZ precipitates out as hydrochloride salt, which was indicated by 4 fold decrease in absorbance (Figure 1c) and by employing microscopy techniques (Figure 1d). Brightfield and positive Cy5 fluorescence confirmed CFZ precipitates as a HCl salt form of the drug; no precipitates were observed for analog 568 (Figure 1d).

Based on the differences in the behavior of CFZ and the 568 analog in the *in vitro* lysosomal microenvironment precipitation assay, we designed experiments to test the behavior of these compounds *in vivo*. After 3-4 weeks of treatment with a drug powder feed diet containing either a dose equivalent of 10mg/kg/day CFZ or analog 568, skin pigmentation was visually evident, which was consistent with observations from previous CFZ studies (Baik et al., 2013). Skin pigmentation in animals was quantitatively determined using 480nm, 535nm, and 623nm optical filters. The reflectance spectra of the skin were compared to that of pure free base and hydrochloride salt solids of CFZ and analog 568 (Figure 2a). Images of CFZ and analog 568 free base and HCl salt forms of the drug powders revealed visual similarities in color and the extent of reflectance at different optical filters (Figure 2a). Both forms of each drug appeared similarly dark in 480nm and 535nm filter images (Figure 2a), supported by high OD values (OD values > 0.5) at those wavelengths (Figure 2c) – making 480nm and

535nm filters ideal for detecting drug-induced skin pigmentation regardless of the drug form. In contrast, 623 nm optical filter distinguished free base from hydrochloride forms of both compounds, with high OD values (OD values > 0.5) indicative of the hydrochloride salt forms and low OD values (OD values < 0.2) indicative of the free base forms (Figure 2c). In this manner, we found that 568 analog treated mice achieved an identical level of pigmentation as CFZ treated mice (no significant difference in OD values (Figure 2b and c)), and both were significantly higher than the untreated group ($p<0.01$, ANOVA Single Factor, Tukey HSD, n=3). Interestingly, use of the 623nm optical filter was unable to detect the skin pigmentation in CFZ and 568 analog treated mice, consistent with the spectra of the free base form of the compounds.

To further elucidate the distribution behaviors of these compounds, the tissues of interest from CFZ and 568 analog treated mice were harvested and cryosectioned for multi-parameter microscopic imaging (Rzeczycki et al., 2017). As previously reported, CLDIs were observed in the liver and spleen of CFZ treated mice based on brightfield images and positive fluorescence and diattenuation signals (Rzeczycki et al., 2017); however, CFZ skin sections did not contain CLDIs. A few dark spots present in both untreated animals and in drug treated animals were attributed to melanosomes, which give mice skin its natural pigmentation (Boissy, 1988, Wu et al., 1997). In contrast to CFZ, all tissues from 568 analog treated animals had no evidence of CLDIs accumulation due to lack of fluorescence and dichroism signal in the liver and spleen, which are the main bioaccumulating organs. Due to the fact that treatment with the 568 analog resulted in significant skin pigmentation, to the same extent as in CFZ treatment, we concluded that the skin pigmentation caused by both CFZ and the 568 analog is not associated with CLDIs bioaccumulation.

Lastly, the extent of drug bioaccumulation in the liver, spleen, and skin of CFZ treated mice was compared. Tissue concentrations of the drug in liver, spleen, and skin were determined to be 2.37 ± 0.62 mg/g, 4.34 ± 0.41 mg/g, and 0.16 ± 0.04 mg/g, respectively. The skin showed significantly lower concentrations compared to liver and spleen ($p<0.001$, ANOVA Single Factor, Tukey HSD, n=3 (skin), n=4 (liver and spleen)). Interestingly, since the skin is the biggest organ, representing 9.8% of total bodyweight (Arms et al., 1988), it accommodated a similar total CFZ mass as the spleen but at a 20 fold lower concentration. This much lower concentration of CFZ in the skin suggests that skin pigmentation is not associated with extensive bioaccumulation of the hydrochloride salt of CFZ and its precipitation into CLDIs, as is observed in liver and spleen. Instead, the lower concentration of CFZ in skin is attributed to the soluble free base form of the drug that is expected to partition into the subcutaneous fat (Baik et al., 2013). In fact, the amount of clofazimine in skin (0.16 mgCFZ/gTissue) is consistent with a ~20% lipid content in skin, assuming that CFZ partitions into skin lipids similarly to the measured concentration that is found in adipose tissue (0.74 mgCFZ/gFat) (Baik et al., 2013).

Overall, in case of oral or systemic administration of CFZ, our results suggest that skin hyperpigmentation should be expected because following absorption, the drug will naturally accumulate in the skin by partitioning from the systemic circulation. Therefore, the most viable alternative approach to reduce CFZ-induced skin hyperpigmentation would be to minimize the concentrations of drug in the circulation. This can be achieved through local

administration and controlled release formulations. In this regard, an inhalable CFZ formulation has already been shown to be efficacious against *Mycobacterium tuberculosis* in human monocyte-derived macrophage cultures and in a relevant animal model (Verma et al., 2013). Based on our own findings, we are currently working towards reformulating CFZ, both as a locally injectable suspension of micronized, biomimetic crystals of CFZ hydrochloride, as well as an inhalable dry micronized powder. By advancing solid, micro or nanoparticles of CFZ that mimic the solid form of the drug that naturally bioaccumulates in CLDIs upon prolonged oral dosing (Baik and Rosania, 2012, Baik et al., 2013, Keswani et al., 2015a), it may be possible to achieve prolonged, therapeutic drug concentrations at the site of action while avoiding CFZ-induced skin pigmentation which would result from high drug concentrations circulating throughout the body. Indeed, while the clinically used, oral formulation of CFZ is specifically indicated to treat leprosy, which primarily affects the skin, more targeted formulations and local delivery routes could be useful to repurpose the drug for other indications.

Materials & Methods

Animal Experiments

All animal care was provided by the University of Michigan's Unit for Laboratory Animal Medicine (ULAM), and the experimental protocol was approved by the Committee on Use and Care of Animals. As per previously established dosage regimen (Baik et al., 2013, Keswani et al., 2015b, Yoon et al., 2016), 4-5 week old Balb/c and C57BL/6 mice from Jackson Laboratory (Bar Harbor, ME) were given an *ad libitum* drug powder feed diet, designed to target oral dose equivalent of 10mg/kg/day CFZ (C8895, Sigma-Aldrich, St. Louis, MO) or CFZ analog 568. Compound 568 was synthesized in bulk using a previously established protocol (Min et al., 2015). After 3-4 weeks of dosing, photographs of mice were taken using iPhone SE camera, the mice were euthanized via CO_2 asphyxiation, and a blood sample was acquired via cardiac puncture. The liver, spleen, and ears were harvested and washed in cold PBS. For microscopy analysis, a portion of each tissue was excised, submerged in optimal cutting temperature (OCT) compound (Sakura Finetek USA, Inc., Torrance, CA) before freezing (-80°C). Cryosectioning was carried out using a Leica 3050S Cryostat (Leica Biosystems Inc., Buffalo Grove, IL) with a section thickness of 5 μm.

Physicochemical Parameters of CFZ and Analog 568

LogP and LogD Determination—To predict pKa values and draw structures of CFZ and 568, ChemAxon MarvinSketch Software (Version 5.12.0) was used. LogP and LogD at pH 7.4 were determined experimentally for CFZ and 568 based on the established protocols from Quigley et al., 1990 for CFZ with minor modifications (Quigley et al., 1990). Briefly, the partition behavior of CFZ and the 568 analog was determined by mixing phosphate buffer at pH 3 and 1-octanol (293245; Sigma-Aldrich, St. Louis, MO) 1:1 (v/v) system at 25°C. The partitioning process was carried out in a thermostatically controlled water bath with magnetic stir bar. Stirring time of 24 hours was considered to be sufficient to produce equilibration. Each compound was introduced in organic solvent at its maximum solubility, and the concentration of drug in organic and aqueous layers was spectrophotometrically determined (285nm; Synergy-2 plate reader; Biotek Instruments, Winooski, VT). CFZ and

568 concentrations were calculated from a standard curve. After concentrations were calculated and the apparent partition coefficient was determined, LogP and LogD at pH 7.4 were determined using equations previously described by Quigley et al., 1990 (Quigley et al., 1990).

CFZ and Analog 568 Hydrochloride Salt Synthesis—To synthesize the hydrochloride salt crystals for CFZ and 568, 7mM drug solution in dimethyl sulfoxide (DMSO) (67-68-5, Fisher Scientific, Fair Lawn, NJ) was added to 1M NH_4Cl in 1:1 (v/v) ratio and left for 24-48 hours at room temperature in the dark. After 24-48 hours, the solution with crystals was washed three times with diminishing concentrations of aqueous NH_4Cl (100mM, 10mM, 1mM) to reduce the amount of chloride in the solution. In between washing steps, samples were centrifuged (2000×g for 10 min at 4°C). After the last wash, crystals were resuspended in MilliQ water and immediately snap frozen in liquid nitrogen then freeze-dried.

Absorbance Profiles of CFZ and Analog 568—To compare absorbance profiles among CFZ free base, 568 free base, CFZ-HCl salt, and 568-HCl salt, samples were dissolved in DMSO at the same concentrations (70μM) and determined spectophotometrically (200-550nm with 5nm steps; Synergy-2 plate reader; Biotek Instruments, Winooski, VT) in a UV 96-well plate (8404; Thermo Scientific, Rockford, IL). Blank DMSO was used to obtain baseline absorbance profile.

Assay for HCl Salt Precipitation—To understand precipitation behaviors and the ability of CFZ and analog 568 to form hydrochloride salts, an *in vitro* assay was developed to mimic lysosomal conditions. Two buffer solutions were made: 10mM sodium acetate buffer (pH 4.5) with 10mM CTAB (Solution A) and 10mM sodium acetate buffer (pH 4.5) with 10 mM CTAB and 100mM NaCl (Solution B). In a UV 96-well plate (8404; Thermo Scientific, Rockford, IL) 1uL of 7mM CFZ/568 in DMSO was added to 99uL of each buffer solution, and the precipitation was observed and quantified. The quantification of hydrochloride salt formation was done spectrophotometrically (2.5 hour of shake cycle - varying speeds, 285nm, Synergy-2 plate reader; Biotek Instruments, Winooski, VT). Buffer solution with DMSO was used for baseline absorbance, and brightfield images of the hydrochloride salt precipitation were obtained based on the protocol described in *Multi-Parameter Microscopic Imaging* section.

Imaging and Quantification of Pigmentation Using Various Optical Filters

Based on the absorbance profiles of CFZ and 568, three available single-band bandpass optical filters were used: 480nm (D480/30×; Chroma, Bellows Falls, VT), 535nm (D535/40m; Chroma, Bellows Falls, VT), and 623nm (FF01-623/24-25; Semrock, Brightline®, Rochester, NY). These filters were attached to an iPhone SE camera for image acquisition. The flash and high dynamic range (HDR) options on the camera were disabled, and the camera editing filters were not applied. Quantification analysis of pigmentation was performed using ImageJ image processing software (Schneider et al., 2012).

Quantification of CFZ in Tissues

Harvested tissues were thawed, weighed, cut, and homogenized by sonication (liver and spleen) and mechanical homogenizer (ear) (Pro200; Pro Scientific Inc., Oxford, CT) in radioimmunoprecipitation assay buffer (RIPA buffer; 89900; Thermo Scientific; Rockford, IL) containing protease inhibitor cocktail (78410; Thermo Scientific; Rockford, IL). Homogenates were centrifuged (15000 rpm at 4°C for 5 min), and the supernatants were collected. The lipophilic tissue fraction was extracted with xylenes (CAS 1330-20-7/100-41-4; Fisher Chemical, Fair Lawn, NJ) in triplicates, followed by the second extraction in triplicates with 9M H_2SO_4 of diprotonated CFZ from the xylenes extract. Samples were centrifuged (2000×g at 4°C for 10 min) to facilitate layer separation during extractions. After acid fractions were collected, the volumes were recorded, and CFZ concentrations were determined spectrophotometrically. The absorbance of the supernatants was measured at λ = 540 nm (A_{540}) and 750 nm (A_{750}) using Synergy-2 plate reader (Biotek Instruments, Winooski, VT). Corrected absorbance (A_{540}-A_{750}) was used to determine CFZ content via a standard curve of standards in 9M H_2SO_4, and the concentration values were corrected for organ weight (Trexel et al., 2017, Yoon et al., 2015). To correct for extraction yield, known amounts of CFZ were added to tissue samples (untreated liver, spleen, and ear tissues) before extractions; these samples were processed and analyzed concurrently with the test samples. For liver and spleen tissues, the extraction yield averaged 90% for skin tissues, the extraction yield averaged 62%.

Multi-Parameter Microscopic Imaging

Multi-parameter polarization, brightfield, and fluorescence microscopy was carried out using a Nikon Eclipse Ti inverted microscope (Nikon Instruments, Melville, NY). Polarization microscopy was performed using the LC-PolScope (Mehta et al., 2013), with the illuminating light narrowed to 623 nm by an interference filter (623±23 nm, FF01-623/24-25; Semrock, Brightline®, Rochester, NY). Polarization images were captured using an Abrio imaging system (Cambridge Research & Instrumentation, Inc, Woburn, MA). Brightfield images were captured using the Nikon DS-3 camera (Nikon Instruments), and fluorescence imaging was done with the Photometrics CoolSnap MYO camera system (Photometrics, Tuscon, AZ) under the control of Nikon NIS-Elements AR software (Nikon Instruments). Illumination for fluorescence imaging was provided by the X-Cite 120Q Widefield Fluorescence Microscope Excitation Light Source (Excelitas Technology, Waltham, MA). An in-depth discussion of this multi-parameter microscopic imaging method was recently described (Rzeczycki et al., 2017).

Statistics

Statistical analysis was performed using SPSS Statistics Software (Version 24; Armonk, New York). Data are expressed as the mean ± SD. A one-way analysis of variance (ANOVA) single factor followed by a Tukey's honest significant difference (HSD) or Games-Howell post hoc tests were used to determine significant differences when applicable.

Acknowledgments

The authors acknowledge support from an M-cubed grant and NIH grant R01 GM078200 to GRR.

References

Arbiser JL, Moschella SL. Clofazimine: a review of its medical uses and mechanisms of action. J Am Acad Dermatol. 1995; 32(2 Pt 1):241–7. [PubMed: 7829710]

Arms, AD., Travis, CC. Health USEPAOo, Assessment E. Reference Physiological Parameters in Pharmacokinetic Modeling. U.S. Environmental Protection Agency, Office of Health and Environmental Assessment; 1988.

Baik J, Rosania GR. Molecular imaging of intracellular drug-membrane aggregate formation. Mol Pharm. 2011; 8(5):1742–9. [PubMed: 21800872]

Baik J, Rosania GR. Macrophages sequester clofazimine in an intracellular liquid crystal-like supramolecular organization. PLoS One. 2012; 7(10):e47494. [PubMed: 23071814]

Baik J, Stringer KA, Mane G, Rosania GR. Multiscale distribution and bioaccumulation analysis of clofazimine reveals a massive immune system-mediated xenobiotic sequestration response. Antimicrob Agents Chemother. 2013; 57(3):1218–30. [PubMed: 23263006]

Belaube P, Devaux J, Pizzi M, Boutboul R, Privat Y. Small bowel deposition of crystals associated with the use of clofazimine (Lamprene) in the treatment of prurigo nodularis. Int J Lepr Other Mycobact Dis. 1983; 51(3):328–30. [PubMed: 6685693]

Boissy RE. The melanocyte, Its structure, function, and subpopulations in skin, eyes, and hair. Dermatol Clin. 1988; 6(2):161–73.

Chakraborty S, Shukla D, Jain A, Mishra B, Singh S. Assessment of solubilization characteristics of different surfactants for carvedilol phosphate as a function of pH. J Colloid Interface Sci. 2009; 335(2):242–9. [PubMed: 19403142]

Dereure O. Drug-induced skin pigmentation. Epidemiology, diagnosis and treatment. Am J Clin Dermatol. 2001; 2(4):253–62. [PubMed: 11705252]

Dooley KE, Obuku EA, Durakovic N, Belitsky V, Mitnick C, Nuermberger EL, et al. World Health Organization group 5 drugs for the treatment of drug-resistant tuberculosis: unclear efficacy or untapped potential? J Infect Dis. 2013; 207(9):1352–8. [PubMed: 22807518]

Gallo CB, Luiz AC, Ferrazzo KL, Migliari DA, Sugaya NN. Drug-induced pigmentation of hard palate and skin due to chronic chloroquine therapy: report of two cases. Clin Exp Dermatol. 2009; 34(7):e266–7. [PubMed: 19438573]

Gopal M, Padayatchi N, Metcalfe JZ, O'Donnell MR. Systematic review of clofazimine for the treatment of drug-resistant tuberculosis. Int J Tuberc Lung Dis. 2013; 17(8):1001–7. [PubMed: 23541151]

Hastings RC, Gillis TP, Krahenbuhl JL, Franzblau SG. Leprosy. Clin Microbiol Rev. 1988; 1(3):330–48. [PubMed: 3058299]

Jamet P, Traore I, Husser JA, Ji B. Short-term trial of clofazimine in previously untreated lepromatous leprosy. Int J Lepr Other Mycobact Dis. 1992; 60(4):542–8. [PubMed: 1299709]

Keswani RK, Baik J, Yeomans L, Hitzman C, Johnson AM, Pawate AS, et al. Chemical Analysis of Drug Biocrystals: A Role for Counterion Transport Pathways in Intracellular Drug Disposition. Mol Pharm. 2015a; 12(7):2528–36. [PubMed: 25926092]

Keswani RK, Yoon GS, Sud S, Stringer KA, Rosania GR. A far-red fluorescent probe for flow cytometry and image-based functional studies of xenobiotic sequestering macrophages. Cytometry A. 2015b; 87(9):855–67. [PubMed: 26109497]

Maia MV, Cunha Mda G, Cunha CS. Adverse effects of alternative therapy (minocycline, ofloxacin, and clofazimine) in multibacillary leprosy patients in a recognized health care unit in Manaus, Amazonas, Brazil. An Bras Dermatol. 2013; 88(2):205–10. [PubMed: 23739719]

Manallack DT. The pK(a) Distribution of Drugs: Application to Drug Discovery. Perspect Medicin Chem. 2008; 1:25–38.

Mehta SB, Shribak M, Oldenbourg R. Polarized light imaging of birefringence and diattenuation at high resolution and high sensitivity. J Opt. 2013; 15(9)

Min KA, Rajeswaran WG, Oldenbourg R, Harris G, Keswani RK, Chiang M, et al. Massive Bioaccumulation and Self-Assembly of Phenazine Compounds in Live Cells. Adv Sci (Weinh). 2015; 2(8)

Quigley JM, Fahelelbom KMS, Timoney RF, Corrigan OI. Temperature-Dependence and Thermodynamics of Partitioning of Clofazimine Analogs in the Normal-Octanol Water-System. International Journal of Pharmaceutics. 1990; 58(2):107–13.

Rzeczycki P, Yoon GS, Keswani RK, Sud S, Stringer KA, Rosania GR. Detecting ordered small molecule drug aggregates in live macrophages: a multi-parameter microscope image data acquisition and analysis strategy. Biomed Opt Express. 2017; 8(2):860–72. [PubMed: 28270989]

Schneider CA, Rasband WS, Eliceiri KW. NIH Image to ImageJ: 25 years of image analysis. Nat Methods. 2012; 9(7):671–5. [PubMed: 22930834]

Singh H, Nel B, Dey V, Tiwari P, Dulhani N. Adverse effects of multi-drug therapy in leprosy, a two years' experience (2006-2008) in tertiary health care centre in the tribal region of Chhattisgarh State (Bastar, Jagdalpur). Lepr Rev. 2011; 82(1):17–24. [PubMed: 21644468]

Stauber T, Jentsch TJ. Chloride in vesicular trafficking and function. Annu Rev Physiol. 2013; 75:453–77. [PubMed: 23092411]

Sukpanichnant S, Hargrove NS, Kachintorn U, Manatsathit S, Chanchairujira T, Siritanaratkul N, et al. Clofazimine-induced crystal-storing histiocytosis producing chronic abdominal pain in a leprosy patient. Am J Surg Pathol. 2000; 24(1):129–35. [PubMed: 10632497]

Tang S, Yao L, Hao X, Liu Y, Zeng L, Liu G, et al. Clofazimine for the treatment of multidrug-resistant tuberculosis: prospective, multicenter, randomized controlled study in China. Clin Infect Dis. 2015; 60(9):1361–7. [PubMed: 25605283]

Trexel J, Yoon GS, Keswani RK, McHugh C, Yeomans L, Vitvitsky V, et al. Macrophage-Mediated Clofazimine Sequestration Is Accompanied by a Shift in Host Energy Metabolism. J Pharm Sci. 2017; 106(4):1162–74. [PubMed: 28007559]

Verma RK, Germishuizen WA, Motheo MP, Agrawal AK, Singh AK, Mohan M, et al. Inhaled microparticles containing clofazimine are efficacious in treatment of experimental tuberculosis in mice. Antimicrob Agents Chemother. 2013; 57(2):1050–2. [PubMed: 23183441]

World Health Organization. [accessed Aug 16.2016] Leprosy Report. 2014. http://www.who.int/mediacenter/factsheets/fs101/en;

Wu X, Bowers B, Wei Q, Kocher B, Hammer JA 3rd. Myosin V associates with melanosomes in mouse melanocytes: evidence that myosin V is an organelle motor. J Cell Sci. 1997; 110(Pt 7): 847–59. [PubMed: 9133672]

Yoon GS, Keswani RK, Sud S, Rzeczycki PM, Murashov MD, Koehn TA, et al. Clofazimine Biocrystal Accumulation in Macrophages Upregulates Interleukin 1 Receptor Antagonist Production To Induce a Systemic Anti-Inflammatory State. Antimicrob Agents Chemother. 2016; 60(6):3470–9. [PubMed: 27021320]

Yoon GS, Sud S, Keswani RK, Baik J, Standiford TJ, Stringer KA, et al. Phagocytosed Clofazimine Biocrystals Can Modulate Innate Immune Signaling by Inhibiting TNFalpha and Boosting IL-1RA Secretion. Mol Pharm. 2015; 12(7):2517–27. [PubMed: 25909959]

Abbreviations

CFZ	clofazimine
CLDI(s)	crystal-like drug inclusion(s)
FDA	Food and Drug Administration
MDR-TB	multi-drug resistant tuberculosis
NSAID	Nonsteroidal anti-inflammatory drug

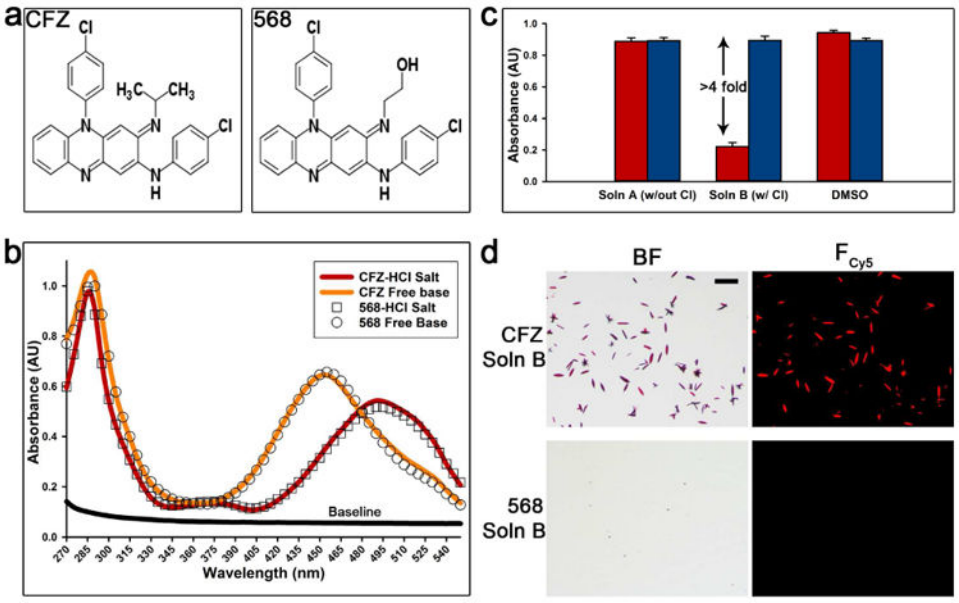

Figure 1. Comparison of CFZ and CFZ analog 568: structures, precipitation assay, and absorbance profiles

(**a**) The structural difference between CFZ and analog 568 at the tertiary amine is a specific substitution of the isopropyl group with a 2-hydroxyethyl. (**b**) The absorbance profiles (270-550nm) show the similarity of CFZ and analog 568 free base and hydrochloride salt forms, respectively. (**c**) The ability of both CFZ and analog 568 to precipitate as hydrochloride salt in simulated lysosomal conditions (pH 4.5). This was determined by measuring the absorbance (285nm) in different conditions: Soln A (no chloride), Soln B (100mM chloride), and DMSO (red = CFZ, blue = 568). (**d**) Hydrochloride salt precipitation in the presence of chloride (Soln B) was verified by brightfield (BF) and fluorescence microscopy (F_{cy5}). Scale bar = 50μm.

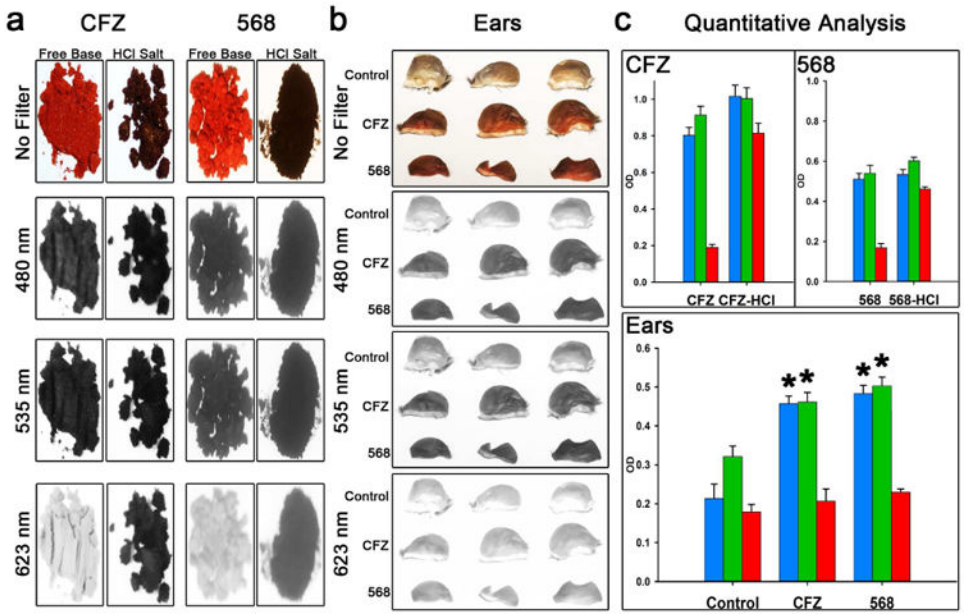

Figure 2. Optical properties of CFZ and CFZ analog 568 and quantitative analysis of skin pigmentation using various optical filters

(**a**) Images of CFZ and analog 568 free base and HCl salt powders and the extent of their reflectance using 480nm, 535nm, and 623nm optical filters. (**b**) Images of mouse ears after 3-4 weeks of CFZ or analog 568 treatment and the extent of their reflectance using 480nm, 535nm, and 623nm optical filters. (**c**) Quantitative analysis of the drug powder images (n=7) and images of mouse ears after 3-4 weeks of CFZ or 568 treatment compared to untreated mice (n=3) (blue = 480nm filter; green = 535nm filter; red = 623nm filter; *p < 0.01, ANOVA single factor, Tukey's HSD).

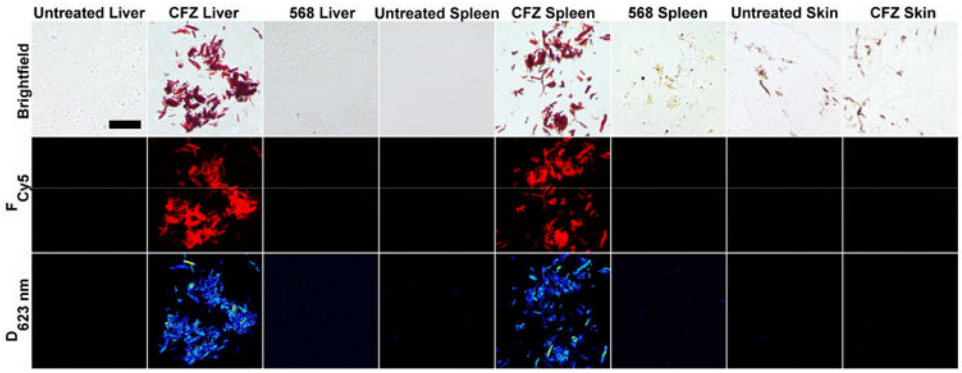

Figure 3. Multi-parameter imaging of CFZ and CFZ analog 568 treated and untreated tissues

Images of liver, spleen, and skin sections were taken using brightfield, Cy5 fluorescence (F_{cy5}), and dichroism at 623nm (D_{623nm}) in order to identify and compare for CFZ-HCl/CLDI signatures with corresponding untreated samples. Scale Bar = 25μm.

Table 1
Physicochemical Parameters of CFZ and 568

	CFZ	568
M.W.	473.4 g/mol	475.4 g/mol
pKa	pKa_1 = 9.29[1]	pKa_1 = 8.65[1]
	pKa = 2.31[1]	pKa = 2.31[1]
LogP	7.66[2]	6.69[2]
LogD @ pH 7.4	5.76[3]	5.42[3]

[1] Values were predicted by ChemAxon MarvinSketch Software (Version 5.12.0)

[2] CFZ mean ± 0.00 (n=3); 568 mean ± 0.04 (n=3)

[3] CFZ mean ± 0.00 (n=3); 568 mean ± 0.04 (n=3)